行政院國家科學委員會補助專題研究計畫 期中進度報告

奈米結構材料在電解水之應用

計畫類別：■ 個別型計畫　　□ 整合型計畫
計畫編號：NSC 98-2221-E-009-040-MY2
執行期間：2009 年 08 月 01 日至 2010 年 07 月 31 日
執行單位：國立交通大學 材料科學與工程學系

計畫主持人：吳樸偉

計畫參與人員：張雲閔、陳境妤、王儷曄

成果報告類型(依經費核定清單規定繳交)：■精簡報告　□完整報告

本成果報告包括以下應繳交之附件：
□赴國外出差或研習心得報告一份
□赴大陸地區出差或研習心得報告一份
□出席國際學術會議心得報告及發表之論文各一份
□國際合作研究計畫國外研究報告書一份

處理方式：本計畫可公開查詢

中　華　民　國　99　年　5　月　31　日

行政院國家科學委員會專題研究計畫 進度報告

奈米結構材料在電解水之應用

計畫編號：NSC 98-2221-E-009-040-MY2
執行期限：2009 年 08 月 01 日至 2010 年 07 月 31 日
主持人：交通大學材料系吳樸偉

摘要

We employed a templated synthetic approach to prepare Ru-Ni inverse opals on a Si substrate. Electrophoretic deposition of polystyrene (PS) microspheres was carried out, followed by electroplating of Ni to fabricate the inverse opal of Ni in nanobowl structure. The nanobowl structure was evaluated for hydrogen evolution reaction (HER) in current-potential polarizations. To further improve the catalytic ability for HER, the Ni nanobowl was subjected to an electroless deposition to prepare a continuous RuO_x film atop the Ni skeleton. After reducing treatment, the RuO_x film was reduced to Ru film. We also performed electrochemical analysis on the Ru-Ni inverse opals for HER abilities.

關鍵字：Electrophoretic deposition; water electrolysis; colloidal crystals

1. Introduction

Water electrolysis is the most straightforward way to produce H_2 and O_2 because water is abundant, and the decomposition of water to H_2 and O_2 electrochemically or photochemically is technically feasible. Despite its simplicity, the large-scaled implementation of water electrolysis is still hindered because of severe polarization loss at both electrodes. Recently, we fabricated the Ni inverse opals (NIOs) in multiple layers and evaluated their electrochemical characteristics for the oxygen reduction reaction (OER) and hydrogen evolution reaction (HER) in an alkaline electrolyte [1]. Due to its chemical inertness, the Ni is known as an electrode support in alkaline electrolyte. Therefore, further enhancement in the HER ability is certainly possible once suitable electrocatalysts are impregnated onto the Ni support. In this work, we prepared the Ni structure in a nanobowl arrangement and explored the deposition of Ru in both metallic and oxide forms atop the Ni inverse skeleton for potential improvements in HER ability.

The motivation for this work is to improve the process for water electrolysis. We realize that the electrochemical generation of H_2 is environmentally friendly. Hence, we attempt to improve the efficiency for HER in order to reduce undesirable energy cost.

2. Experimental

The detailed processing steps for the NIOs have been described elsewhere [1]. A simple

schematic is shown in Fig. 1 and a brief description for the steps involved is provided below. A 6-inch (100) Si wafer of low resistivity (<0.01 Ω-cm) was used as the substrate. First, the Si substrate underwent a wet thermal process to form 600 μm SiO_2 layer on surface. The purpose for the thin SiO_2 layer was to serve as an insulating film to isolate conductive area for following steps. Afterward, a Ti thin film of 500 nm thickness was deposited on top of the SiO_2 layer by electron beam evaporation technique. Subsequently, electrophoresis of PS microspheres in 660 nm diameter was imposed to fabricate PS colloidal crystal. The electrophoresis was performed at 10 V/cm^2 for 5~60 min. Next, the Ni was electroplated into the interstitial voids among the PS microspheres at ~300 nm height. The electrolyte for the Ni plating included 130 g/L of $NiSO_4 \cdot 6H_2O$, 30 g/L of $NiCL_2 \cdot 6H_2O$, 18 g/L of H_3BO_3, and 3 mL of H_2O_2. The electrodeposition of Ni was carried out under 0.4 V/cm for 20 min. The bath temperature was kept at 25 ^oC at pH of 5.2. Finally, the PS microspheres were carefully removed at 250 ℃ for 24 h.

For the electroless deposition of Ru thin film on the NIOs substrate, the NIOs substrate underwent an activation treatment by submerging in an aqueous solution including 0.1 wt% $PdCl_2$ (Aldrich) and 1 wt% HCl (SHOWA) for 10 s. Subsequently, the activated NIOs substrate was immersed in the plating bath which contained 30 mL of aqueous solution consisting of 0.0186 g $K_2RuCl_5 \cdot xH_2O$ (Alfa Aesar), 0.0704 g $NaNO_2$ (SHOWA), 0.04 g NaOH (Mallinckrodt), and 1.8858 g NaClO (SHOWA). Both the activation step and electroless deposition process were conducted at 40 ℃. Afterward, the sample was kept in the plating solution for 40 min and dried in air. To prepare a pure Ru film, we also performed a reduction treatment on the sample at 100~200 ℃ for 2 h under pure H_2 condition.

In electrochemical analysis, an aqueous solution of 1 M KOH was used. A three-electrode configuration was adopted where the reference electrode was a Ag/AgCl electrode with saturated KCl, and the counter electrode was a Pt foil (6.25 cm^2). The Ru-NIOs with a geometric area of 1 cm^2 was fastened by a Teflon holder serving as the working electrode. Electrochemical measurements in current-potential polarizations (*i*-V) were conducted by a Solartron SI1287 with a scan rate of 1 mV/sec for -0.2 to -1.8 V at 25 ˚C.

Field-emission Scanning Electron Microscope (FE-SEM; JEOL-JSM-6700F) was used to observe the morphologies for the Ru-NIOs structure. Energy dispersive X-ray (EDX) analysis was adopted to analyze the composition for the Ni and Ru. X–ray Photoelectron Spectroscopy (XPS; Thermo Microlab 350) was used to confirm the oxidative states of Ru in the Ru-NIOs structure.

3. Results and discussion

The fabrication of PS colloidal crystals by electrophoretic deposition has been demonstrated by many research groups. Figure 2 demonstrates the typical behavior of current density variation during the electrophoresis process. As shown, the current density for the working electrode was found to decrease with increasing deposition time. This was attributed to the “shielding effect” where the electrical field was gradually reduced once the PS

microspheres were assembled on the substrate.

Figure 3(a) and 3(b) provide the SEM images for the samples prepared by the electrophoresis process with different deposition times. As expected, the PS microspheres are packed properly to form colloidal crystals in multiple layers for 3 and 6 min. The relevant time dependence of PS microspheres thickness is displayed in Fig. 4. It can be concluded that the packing velocity for the PS microspheres decreased with increasing electrophoresis time, a behavior consistent to what we observed in Fig. 2.

Figure 5 provides the SEM images in both top and cross-sectional view for the semi-layer NIOs. After removing PS microspheres, the electrodeposited Ni formed a continuous network of pores in a hexagonal arrangement, the exact replica for a close-packed fcc lattice. The average diameter for the bowl-like structure was consistent to that of the PS microspheres. In cross-sectional view, the bowl-like structure is clearly visible.

Figure 6 exhibits the SEM images for the electroless-deposited RuO_x on the NIOs structure at electroless deposition time of 0.5, 2, and 4 hr, respectively. As expected, the diameter for the pore was reduced gradually with increasing deposition time. In addition, results from EDX confirmed the nature of RuO_x, in which an increasing Ru percentage was recorded with prolonged deposition time, shown in Fig. 7.

Figure 8(a) exhibits the HER *i*-V curves for the RuO_x-NIOs with various electroless deposition time of 0.5, 2, and 4 hr, respectively. The *i*-V behavior for the NIOs was also evaluated as a reference. The open circuit voltage started at an equilibrium potential of -0.2 V (vs. Ag/AgCl), and the current response was recorded when the applied potential became more cathodic. The current values demonstrated notable increments when the cathodic potential reached -1.0 V. As expected, the RuO_x-NIOs revealed an improved HER ability compared with that of NIOs. Among these samples, the RuO_x-NIO with 2 hr electroless deposition revealed the largest catalytic ability. Shown in Fig. 8(b) is the comparison of current density at -1.8 V.

The SEM images for the RuO_x-NIOs before and after H_2 treatment are presented in Fig. 9(a) and 9(b). Before H_2 treatment, the RuO_x-NIOs surface was rather irregular as shown in Fig. 9(a). In contrast, a much smoother surface was obtained after the annealing treatment, as shown in Fig. 9(b).

Figure 10(a) and 10(b) provide the XPS analysis from Ru 3p on the RuO_x-NIOs before and after H_2 treatment. To determine the relative ratios quantitatively, the curve fitting by Avantage software was carried out. The corresponding peaks for Ru, $RuO_2 \cdot nH_2O$, and RuO_3 were 462.2, 463.8 and 466.9 eV, respectively [2]. As shown in Fig. 10, we found that the ratio for the metallic Ru was increased after H_2 treatment. However, the remaining presence of RuO_x was attributed to the surface Ru which was known to oxidize easily upon exposure to ambient. The complete synthetic parameters and numeric results are listed in Table I.

Figure 11 demonstrates the HER *i*-V curves for the RuO_x-NIOs with 2 hr of Ru electroless deposition and various H_2 treatments. The NIOs is also included as a reference. At 200 ℃ of H_2 treatment, the electrode revealed impressive activities for

HER. When the calcination temperature was increased, we obtained improved crystallinity and larger grain sizes. It is known that the extent of crystallinity plays a critical role in the resulting electrocatalytic activity. Again, the metallic Ru revealed better electrocatalytic activity than that of RuO_x in the HER process.

4 Conclusions

In summary, experimental work has been carried out to prepare PS colloidal crystals in multiple layers followed by electroplating of Ni to fabricate NIOs in nanobowl structure. The NIOs and catalyzed NIOs (via electroless Ru/RuO_x deposition) were evaluated for HER abilities. Results from *i*-V polarizations indicated that the catalytic abilities for HER were improved considerably once RuO_x-NIOs and Ru-NIOs were formed. Furthermore, the Ru-catalyzed structure revealed better performance than that of RuO_x-catalyzed one.

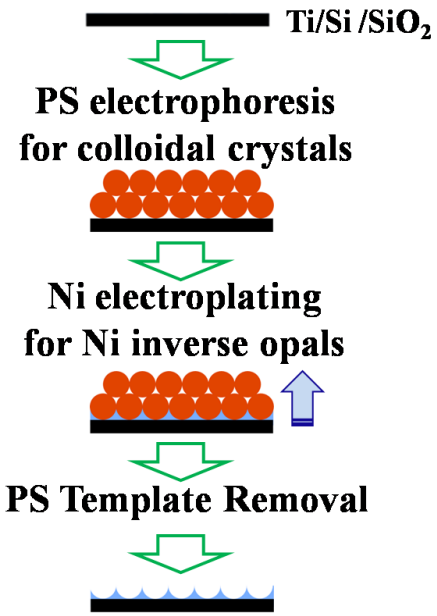

Fig. 1: Experimental flowchart for the steps involved in the preparation of NIOs substrate.

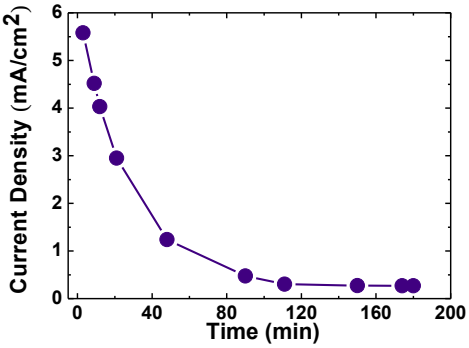

Fig. 2: The time dependence of current density during electrophoresis of PS microspheres.

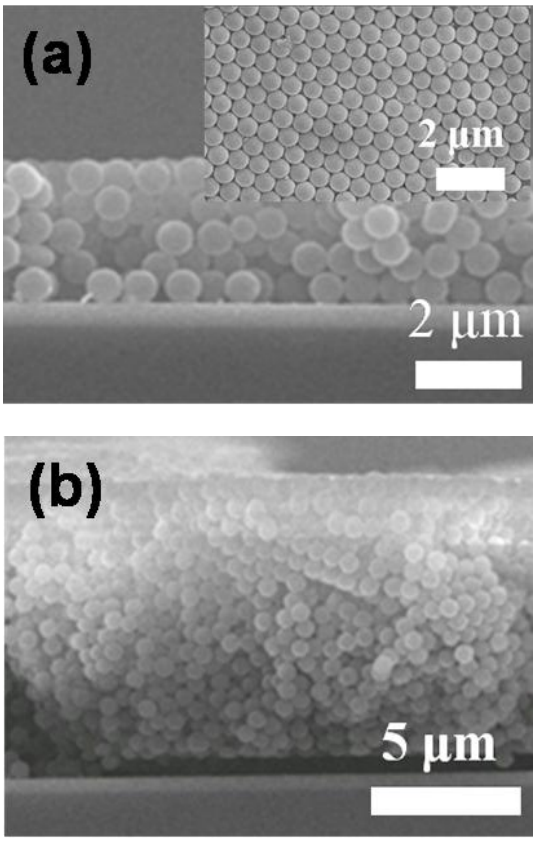

Fig. 3: The SEM images of PS microspheres deposited at 10 V/cm for (a) 3 and (b) 6 min. The inset is the respective top-view image.

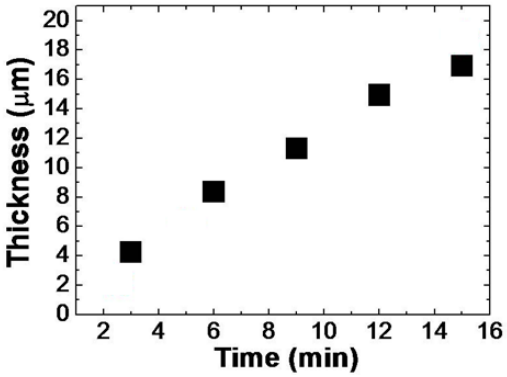

Fig. 4: The variation of PS colloidal crystals thickness as a function of electrophoresis time.

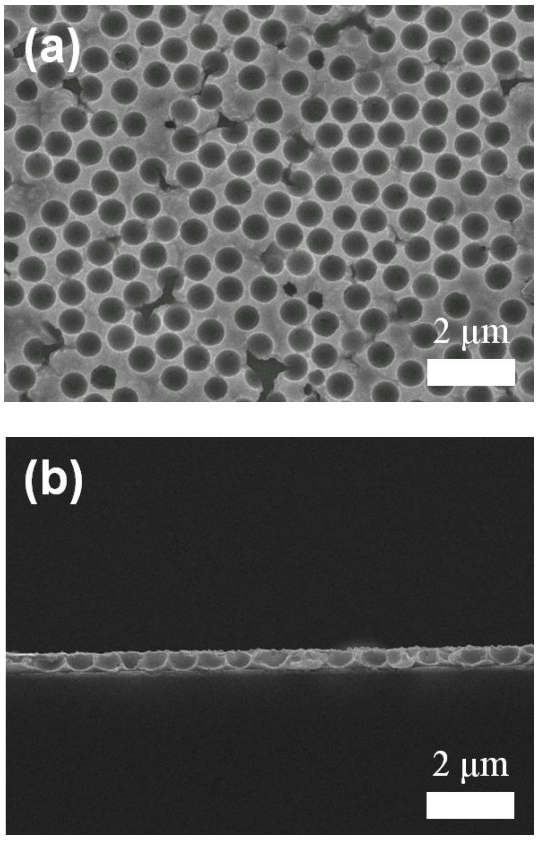

Fig. 5: The SEM images in (a) top and (b) cross-sectional view for the NIOs in a nanobowl structure.

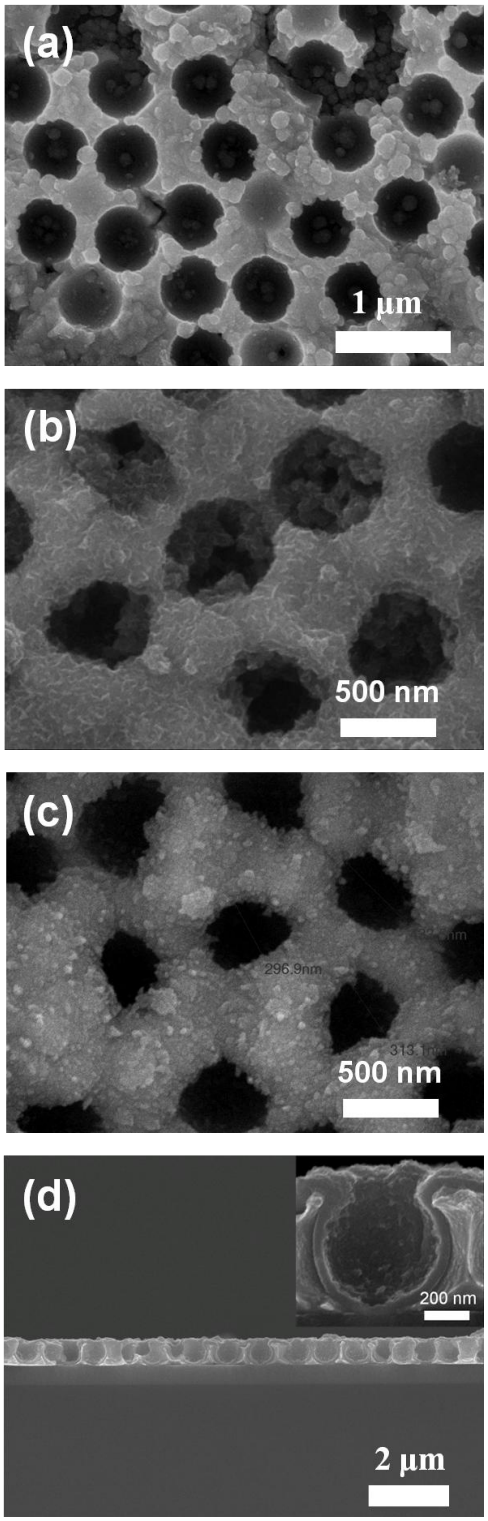

Fig. 6: Top-view SEM images for RuO_x-NIOs undergoing electroless deposition time of (a) 0.5, (b) 2, and (c) 4 h, respectively. (d) is the cross-sectional view of RuO_x at 2h, and its inset is the same sample with higher magnification, showing a conformal coverage of RuO_x.

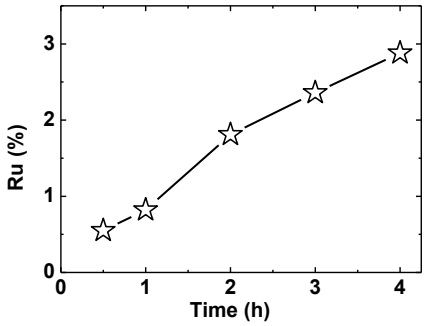

Fig. 7: The variation of Ru amount for different electroless deposition time.

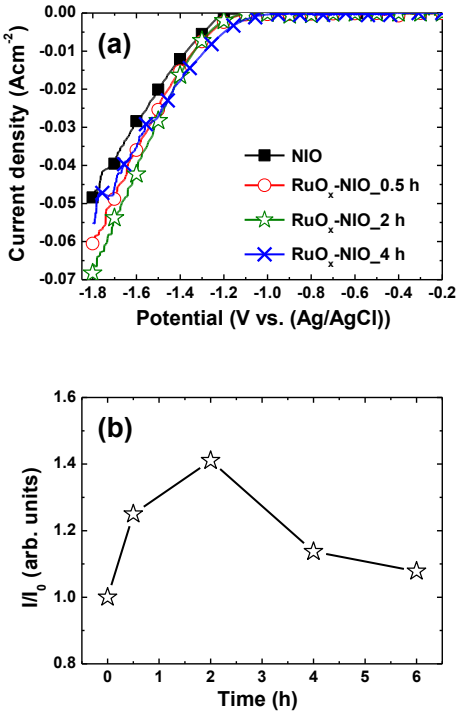

Fig. 8: (a) The HER *i*-V curves for the NIOs as well as RuO_x-NIOs with electroless deposition time of 0.5, 2, and 4 hr, respectively. (b) is the deposition time dependence of current density ratio at -1.8 V.

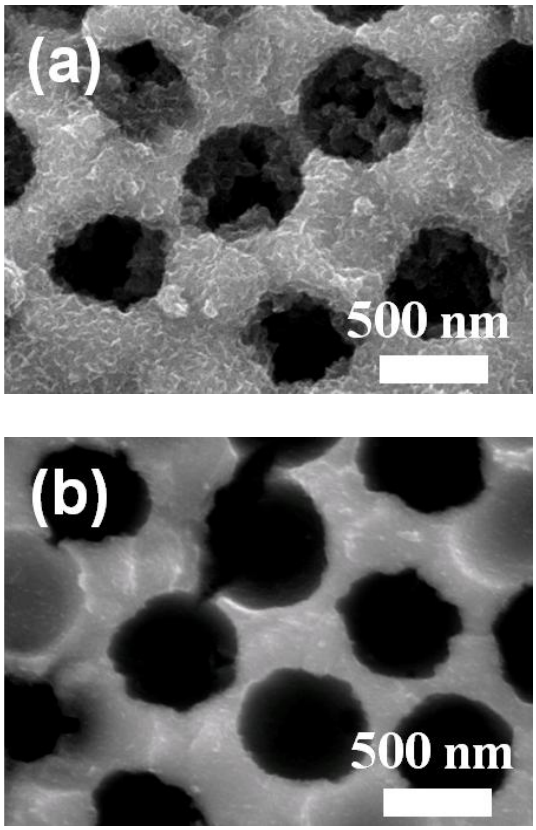

Fig. 9: The SEM images of RuO_x-NIOs in (a) before and (b) after 2 h H_2 treatment.

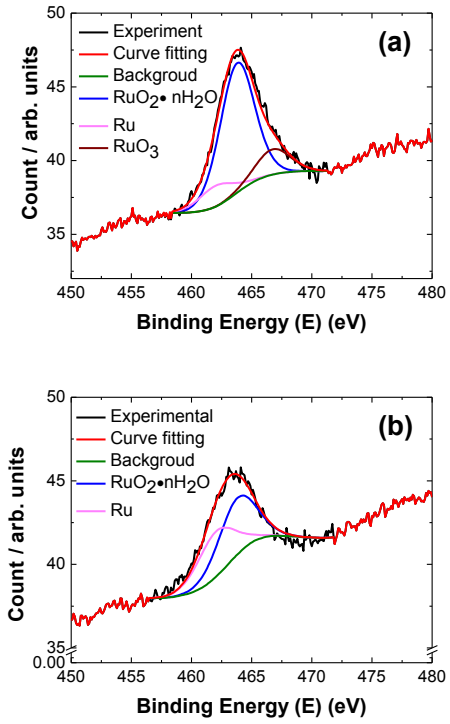

Fig. 10: The XPS signals for Ru 3p in (a) before and (b) after H_2 treatment.

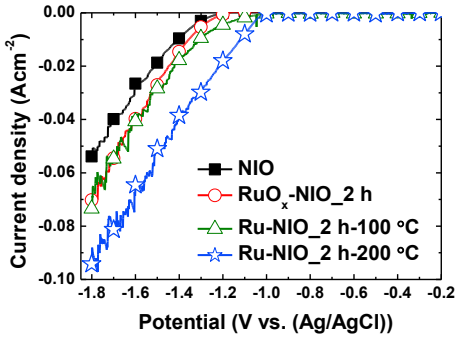

Fig. 11: The HER *i*-V curves for NIOs, RuO_x-NIOs deposition time of 2 hr, as well as Ru-NIOs before and after H_2 annealing.

Table I. Results from XPS and curve fitting of RuO_x-NIOs before and after H_2 annealing.

	Binding energy[a)] (eV)	Peak area (eV)	Suggested species	Area ratio (%)
Before	463.79	32046.71	RuO_2•nH_2O	74
	462.03	5184.86	Ru	12
	466.76	6254.25	RuO_3	15
After	463.79	13379.3	RuO_2•nH_2O	55
	462.04	10726.72	Ru	45
	-	-	RuO_3	-

a) from XPS curve fitting

5. References

1. Y.J. Huang, C.H. Lai, P.W. Wu, and L.Y. Chen, J. Electrochem. Soc., ***157*** (3), P18-P22 (2010).
2. NIST X-ray Photoelectron Spectroscopy Database, Version 3.5 (National Institute of Standards and Technology, Gaithersburg,2003); http://srdata.nist.gov/xps.

6. 計畫成果自評

We have completed the following tasks successfully during the first-year of this two-year project.

- Exploration of AAO processing parameters to obtain pore channels with distinct pore diameters.
- Fabrication of Ni nanowires in various aspect-ratios and inter-nanowires distances.
- Electrophoretic depositions of microspheres using SiO_2 and PS in various sizes and controlled their assembly in multiple layers.
- Construction of Ni nanobowls in different voids and layers.
- Characterizations for materials properties such as XRD, SEM, XPS, and EDX for the Ni nanowires and nanobowls.
- Electrochemical analysis for hydrogen evolution reaction in various KOH electrolytes and temperatures.